

RSC Advances



This is an *Accepted Manuscript*, which has been through the Royal Society of Chemistry peer review process and has been accepted for publication.

Accepted Manuscripts are published online shortly after acceptance, before technical editing, formatting and proof reading. Using this free service, authors can make their results available to the community, in citable form, before we publish the edited article. This *Accepted Manuscript* will be replaced by the edited, formatted and paginated article as soon as this is available.

You can find more information about *Accepted Manuscripts* in the [Information for Authors](#).

Please note that technical editing may introduce minor changes to the text and/or graphics, which may alter content. The journal's standard [Terms & Conditions](#) and the [Ethical guidelines](#) still apply. In no event shall the Royal Society of Chemistry be held responsible for any errors or omissions in this *Accepted Manuscript* or any consequences arising from the use of any information it contains.

ARTICLE

Fabrication of Magneto-Responsive Microgears Based on Magnetic Nanoparticles Embedded PDMS

Cite this: DOI: 10.1039/x0xx00000x

Ivna Kavre,^a Gregor Kostevc,^a Slavko Kralj^{b,c} Andrej Vilfan^d and Dušan Babič^a

Received 00th January 2012,

Accepted 00th January 2012

DOI: 10.1039/x0xx00000x

www.rsc.org/

We present a new fabrication method for nonspherical magnetically responsive microparticles. It is based on photo- and soft-lithography and is suitable for production of prism shaped magnetic microparticles. Approximately 10^5 particles per run can be produced. The key element of the fabrication is the soft polydimethylsiloxane (PDMS) mold with hollows obtained by replica molding from a hard (SU-8 photoresist) master. The master is microfabricated by photolithography. The PDMS mold is filled with commercially available magnetic PDMS followed by the addition of superparamagnetic nanoclusters which enhance the magnetic susceptibility of the particles. After the cross-linking process particles are extracted from the mold and dispersed in the water. A magneto-responsive behavior of so produced microparticles is demonstrated in an experiment with magnetic microgears subjected to a rotating magnetic field of different strengths and frequencies. At low frequencies a microgear follows the rotation of the field whereas above the critical frequency the microgear rotation frequency decreases with increasing field frequency. Observed dependence is well explained with a model assuming that the magnetic torque on a microgear results from an anisotropic effective susceptibility as well as finite relaxation time of the magnetization. We also demonstrate that a magnetic microgear can transmit rotation to one or several non-magnetic microgears.

I. Introduction

Miniaturization presents a challenge in many areas of science and technology. There are two main advantages of the miniaturization process: cost and time optimisation. A substantial potential for miniaturization lies in the application of magnetic microparticles in different fields including medicine (bioimaging, biosensing, tissue repair, transport of drugs and nucleic acids),^[1-4] materials science (fabrication of photonic crystals and microdisplays),^[5-8] microfluidics (fabrication of nanomotors and nanomachines),^[9-12] colloidal matter (building blocks for self-assembly or model for biological systems),^[13,14] etc. For these applications mass production of magnetic microparticles with precise control over their size, shape and composition is required.

In most experiments up-to-date colloids containing hard-walled spherical particles interacting either via isotropic or anisotropic interactions were used. For example spherical microparticles have been used as a model system for problems from statistical physics,^[15,16] as functional units in microfluidic devices,^[17] and as building blocks of self-assembled materials.^[18] As a natural follow up the number of experiments with nonspherical microparticles is increasing.^[19-22] In these experiments a

particle shape presents an additional degree of freedom, potentially leading to a richer and thus more complex behavior. Nonspherical magnetic microparticles can be fabricated both by bottom-up and by top-down approaches. There are very few examples of fabrication by bottom-up methods^[23,24] while top-down methods include approaches employing templating and photolithography.^[25-30]

In this paper we present a method based on photolithography^[31,32] and soft-lithography^[33-36] which offers a possibility of producing prism shaped magnetic microparticles using a thermocurable material, polydimethylsiloxane (PDMS) which is one of the most widely used silicon-based organic polymers in soft-lithography. With proper chemical treatment a PDMS can be made magnetic and thus the method can be used to produce magnetic or non-magnetic microparticles.

II. Experimental

A Fabrication of magnetic PDMS microparticles

In this section we describe in detail the microparticle fabrication method. The process is schematically illustrated in Fig.1 and Fig. 2

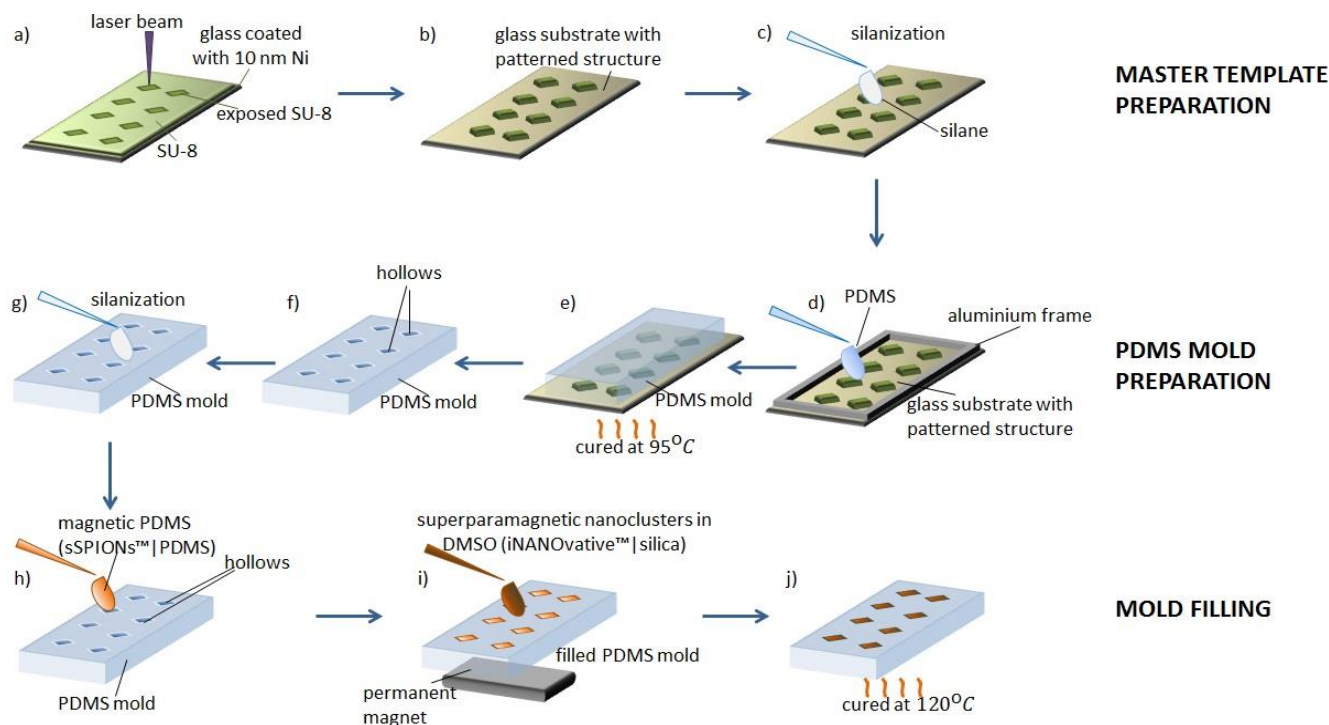


Figure 1. Fabrication of prism shaped magnetically responsive microparticles: schematic representation of the master template preparation, PDMS mold preparation and mold filling.

A1 Master template preparation. The master template consists of an array of SU-8 structures on a glass surface. It is produced as follows:

- The SU-8 master with the desired patterned structure is fabricated by maskless photolithography, using a micropatterning device based on the direct laser imaging (LDI) system – LPKF ProtoLaser D.^[32] Besides the quick pattern illumination this approach allows a design of different patterns in relatively short time (much shorter than the time needed for fabricating a new mask). A photoresist is applied on a substrate (glass slide) by standard spin-coating technique forming a film (~9 μm height – see ESI_1). For improved adhesion the slide is precoated with a thin (10 nm) layer of nickel deposited by sputtering^[37] (Fig. 1a).
- After exposure, the sample is developed (2 minutes, mr-Dev 600 developer, MicroChemicals) and hardbaked (180°C, 1 hour) producing a mechanically and chemically stable pattern required for the mold fabrication (Fig. 1b).
- Before PDMS mold preparation, the template surface is silanized (Octadecyldimethyl (3-trimethoxysilylpropyl) ammonium chloride; 60% in methanol; ABCR GmbH & Co. KG) in order to facilitate separation of the cured PDMS mold from the patterned substrate (Fig. 1c).

A2 Mold preparation. The mold is made of PDMS and contains microhollows (~9 μm depth) obtained by replica molding from the SU-8 photoresist master template. It is prepared as follows:

- An aluminium frame (length: ~20 mm, width: ~20 mm, height: ~10 mm, thickness: ~3mm; see ESI_2) is placed on the master template around the structure and filled with

uncured PDMS to obtain a cuboid shaped mold for the ease of use (Fig. 1d).

- The sample is baked (90-95°C, 20-30 min) (Fig. 1e).
- After PDMS cross-linking, the mold is peeled from the master template and is a negative replica of the master structure (Fig. 1f).
- Before filling the microhollows, the mold is silanized for easier release of the microparticles from the mold (Fig. 1g).

A3 Mold filling. Once the mold is prepared, the microhollows are filled:

- A droplet (30 μl) of commercial magnetic PDMS (sSPIONs™|PDMS) is deposited onto a PDMS mold and the excess material is carefully removed (Fig. 1h). The magnetic PDMS is composed of superparamagnetic maghemite nanoparticles homogeneously dispersed in viscous PDMS and is stable from chemical and colloidal point of view (see ESI_3).
- The magnetic susceptibility of microparticles prepared with solely the magnetic PDMS is too small to observe interparticle magnetic interaction in an external magnetic field of the order few mT (see ESI_3). To enhance their magnetic responsiveness the process is supplemented with the additional step of magnetic doping: a droplet (50 μl) of superparamagnetic nanoclusters (iNANOvative™|silica) dispersed in dimethyl sulfoxide (DMSO) is deposited over the structure in PDMS mold (see ESI_3). The mold is then placed on top of a permanent magnet ($B=1\text{T}$, 15 minutes) to magnetically attract the nanoclusters from DMSO into the magnetic PDMS (Fig. 1i).

- The mold is then cured on a hot plate (120°C, 3 hours minimum) (Fig. 1j).
- After curing the excess material is carefully removed (Fig. 2a).

A4 Release of the particles and experimental cell preparation.

The particle release process is based on different adhesion strengths between the particles and diverse substrates (e.g. particles-PDMS, particles-AZ photoresist, particles-PVA layer) – schematically shown in Fig. 2. In order to prepare the experimental cell magnetic microparticles have to be dispersed in the water and enclosed into the sample cell. The process is as follows:

- PDMS mold is treated with plasma (3 min) in order to activate the particles' surface and a droplet (12-15 μl) of positive photoresist (AZ1505, MicroChemicals) is deposited on the mold (Fig. 2b).
- The mold is pressed against a glass slide and cured on a hotplate (95°C, 60 min). After cooling the mold is gently removed leaving photoresist with an array of microparticles sticking to its surface (Fig. 2c).
- A droplet (30 μl) of 10% aqueous PVA (polyvinyl alcohol, 87-89% hydrolyzed, Sigma Aldrich) is deposited on the structure and the sample is heated on a hotplate (65°C, 20 min) - water evaporates and the PVA layer solidifies (Fig. 2d).
- The PVA layer containing microparticles is peeled from the substrate. Subsequently the microparticles are released by dissolving PVA in water (500 μl). To prevent particle agglomeration, a 2% BSA (bovine serum albumin, Aldrich) solution is used (Fig. 2e).
- The resulting PVA/water solution is exchanged with ultraclean water by sedimenting the microparticles at the bottom of the centrifuge tube and replacing the upper volume of the liquid. Sedimentation is performed using a permanent magnet (Fig. 2f).
- The water mixture of microparticles ($\sim 9 \mu\text{m}$ height, see ESI_1) is used to fill the experimental cell (consisting of spacers and cover glass) by capillary action. Subsequently the experimental cell is sealed with UV glue to prevent evaporation and possible currents. (Fig. 2g and 2h).

- Since the magnetic microparticles are fabricated with magnetic PDMS and superparamagnetic nanoclusters, the saturation magnetization of the doped magnetic PDMS lies between the values of the saturation magnetization of magnetic PDMS (6.2 emu/g) and the one of superparamagnetic nanoclusters (43.2 emu/g) and is approx. 15.4 emu/g. Furthermore, the microparticles demonstrate no remanent magnetization and no coercivity field at room temperature (see ESI_3).

B Fabrication of non-magnetic SU-8 microgears

The SU-8 microgears are fabricated by maskless photolithography (like the master template for mold preparation) on a standard glass slide coated with a thin layer of Ni. The purpose of the Ni layer is to enable the non-destructive release of the particles from the substrate by etching. The lift-off is achieved with a droplet (50 μl) of etchant, which is left on the structure (20 min) to completely dissolve the Ni layer. The floating particles are picked up with a pipette and placed in a centrifuge tube. The etchant is exchanged with water by sedimenting the particles at the bottom of the tube by centrifugation and replacing the upper volume of the liquid. This process is repeated 4 times. To prevent particle agglomeration, 500 μl of 2% BSA solution is added.

C Experimental set-up

The experimental set-up consists of laser tweezers and a magnetic system that generates a rotating magnetic field. Laser tweezers are built around a commercial inverted optical microscope (Zeiss Axiovert 200M, Achroplan 63/0.9W) and are composed of a Nd:YAG laser, acousto-optic deflectors and a beam steering controller (Aresis Tweez). The laser tweezers are used only for positioning of individual microparticles and are switched off during the measurements.

The magnetic system consists of three orthogonal pairs of coils in approximately Helmholtz configuration (for x, y and z directions) powered by a 6-channel computer-controlled current source. The magnetic system offers the possibility to generate rotating magnetic field of adjustable strength and rotation frequency (max 10 mT, 300 Hz).

III. Results and discussion

A Experiments

In Section II we described a method for fabricating non-spherical magnetic microparticles. To demonstrate their application potential we carried out an experiment with magnetic and non-magnetic microgears in aqueous dispersion (Fig. 3b, 3c and 3d).

The sample containing microgears dispersed in water was placed above the microscope objective in the center of the magnetic system's coil configuration (Fig. 3a, ESI_4). The substrate was patterned with SU-8 micropillars which served as axes for the microgears. The experiments were performed with one magnetic microgear (9 or 11 teeth, 39 μm and 46 μm in

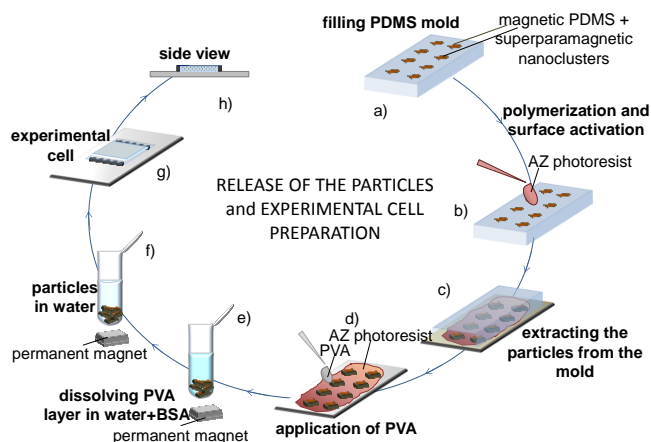


Figure 2. Final steps in the microparticle fabrication process: release of the particles and experimental cell preparation.

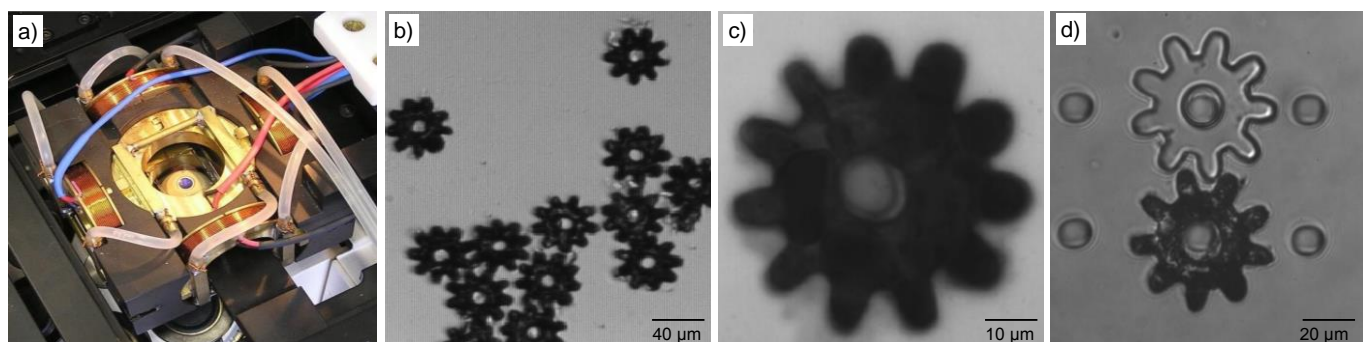


Figure 3. a) Experimental set-up, b)-d) bright field image of microgears in aqueous dispersion: b) small magnetic microgears (9-tooth), c) larger magnetic microgears (11-tooth), d) magnetic (black) and non-magnetic (transparent) microgears on SU-8 micropillars.

diameter and 8 μm thick respectively) and with a pair of microgears: one magnetic and one non-magnetic. In both cases dependence of the microgear rotation frequency was measured as a function of the magnetic field strength and its rotation frequency.

At low frequencies the microgear follows the rotation of the field. Above a critical frequency phase slippage occurs and the rotation frequency decreases with increasing field frequency. A similar effect was reported for particles in ferrofluids,^[38] paramagnetic ellipsoids,^[39] and beads with a permanent magnetic moment.^[40]

Fig. 4a shows the trajectory of a rotating microgear as a function of time and Fig. 4b its angular velocity as a function of the angle between the field and the gear. The latter clearly shows a half-turn periodicity which indicates that the driving torque is caused by an anisotropic susceptibility. A permanent magnetic moment would, on the contrary, show a full turn periodicity. The angular velocity also shows a small bias in the direction of the rotating field, which can be attributed to magnetic relaxation^[38] and becomes stronger at higher frequencies.

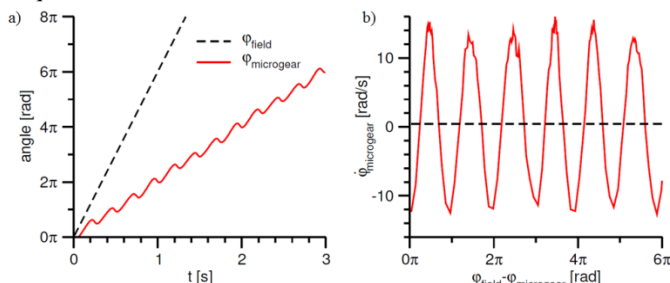


Figure 4. Trajectories of a rotating 9-tooth microgear, ($f_{\text{field}} = 3 \text{ Hz}$, $B = 1.5 \text{ mT}$). a) Orientation angles of the microgear and the magnetic field as a function of time. b) The angular velocity of the microgear as a function of the angle between the field and the microgear. A period of π reveals that the torque on the microgear is caused by an anisotropy in the susceptibility. A small bias in the direction of the rotating field (dashed line) is caused by the relaxation of magnetization.

B Theoretical model

To understand the rotation of microgears we propose a model based on the following assumptions:

- i) The angular velocity of a microgear in viscous environment is proportional to the magnetic torque acting on it:^[41]

$$\dot{\phi}_{\text{microgear}} = \frac{M}{\gamma} \quad (1)$$

- ii) If one aligns the coordinate system with the axes of magnetic anisotropy of a gear, the magnetization caused by a static field is

$$\vec{m} = \frac{\chi V}{\mu_0} \left((1 + \varepsilon) B_x \hat{e}_x + (1 - \varepsilon) B_y \hat{e}_y \right), \quad (2)$$

where ε is a dimensionless measure of anisotropy.^[42] With $\vec{B} = B(\cos\alpha, \sin\alpha, 0)$ the contribution Eq. (2) to the torque on the particle is

$$M_A = \frac{\chi V}{\mu_0} \varepsilon B^2 2\sin(2\alpha). \quad (3)$$

- iii) The magnetization responds to a time dependent field with a relaxation rate $1/\tau$:

$$\vec{m}(t) = \frac{\chi V}{\mu_0 \tau} \int_{-\infty}^t \exp\left(-\frac{t-t'}{\tau}\right) \vec{B}(t') dt'. \quad (4)$$

The following derivation also remains valid if the expression contains a weighted sum of several relaxation processes with different time constants. In the limit of fast relaxation, $\tau \rightarrow 0$, one can use a linear approximation for $B(t')$ and eq. (4) simplifies to

$$\vec{m}(t) = \frac{\chi V}{\mu_0} (\vec{B}(t) - \tau \dot{\vec{B}}(t)). \quad (5)$$

The resulting torque is

$$M_R = \frac{\chi V}{\mu_0} B^2 \tau \dot{\alpha}. \quad (6)$$

In the limit of a weak anisotropy and fast relaxation the contributions are additive. If the field is rotating such that its direction is given by $\phi_{\text{field}} = \omega t$, the sum of both torques M_A and M_R induces a rotation rate

$$\dot{\phi}_{\text{microgear}} = \frac{\chi V B^2}{\mu_0 \gamma} \left(2\varepsilon \sin(2(\omega t - \phi_{\text{microgear}})) + \tau(\omega - \dot{\phi}_{\text{microgear}}) \right), \quad (7)$$

which can be written as

$$\dot{\phi}_{\text{microgear}} = \omega_0 \sin(n(\omega t - \phi_{\text{microgear}})) + R(\omega - \dot{\phi}_{\text{microgear}}) \quad (8)$$

with $n = 2$. Alternatively, if the torque were caused by a permanent magnetic moment, its dynamics would be governed by the same equation with $n = 1$. By substituting $\phi = n(\omega t - \phi_{\text{microgear}})$ one obtains the equation

$$\dot{\phi} = \frac{n\omega_0}{1 + R} \left(\frac{\omega}{\omega_0} - \sin\phi \right). \quad (9)$$

For $\omega < \omega_0$ a phase locked solution, $\phi = \text{const}$ exists and the microgear follows the rotation of the field. Above the critical frequency, phase slippage occurs and the time in which the gear stays behind the field by one period ($1/n$ turn) can be expressed as

$$T = \frac{1+R}{n\omega_0} \int_0^{2\pi} \frac{d\phi}{\omega/\omega_0 - \sin\phi} = \frac{1+R}{n} \frac{2\pi}{\sqrt{\omega^2 - \omega_0^2}} \quad (10)$$

In this time the gear rotates by $\Delta\phi_{\text{microgear}} = \omega T - \frac{2\pi}{n}$ and its average angular speed is

$$\omega_{\text{microgear}} = \frac{\Delta\phi_{\text{microgear}}}{T} = \omega - \frac{2\pi}{nT} = \omega - \frac{1}{1+R} \sqrt{\omega^2 - \omega_0^2} \quad (11)$$

Alternatively, the rotation frequency of the microgear can be expressed as

$$f_{\text{microgear}} = \begin{cases} f_{\text{field}} - \frac{1}{1+R} \sqrt{f_{\text{field}}^2 - f_0^2} & f_{\text{field}} > f_0 \\ f_{\text{field}} & f_{\text{field}} \leq f_0 \end{cases} \quad (12)$$

This equation will be used to fit the measured frequencies as a function of the field frequency. Without the relaxation term ($R = 0$) it becomes identical to that derived in [38].

C One magnetic microgear

We measured the average rotation frequency of a small (9 teeth) and a larger (11 teeth) microgear for different field strengths (1, 1.5 and 2 mT), as a function of the applied field frequency (Fig. 5) (ESI_5: movie1-movie4). The data were

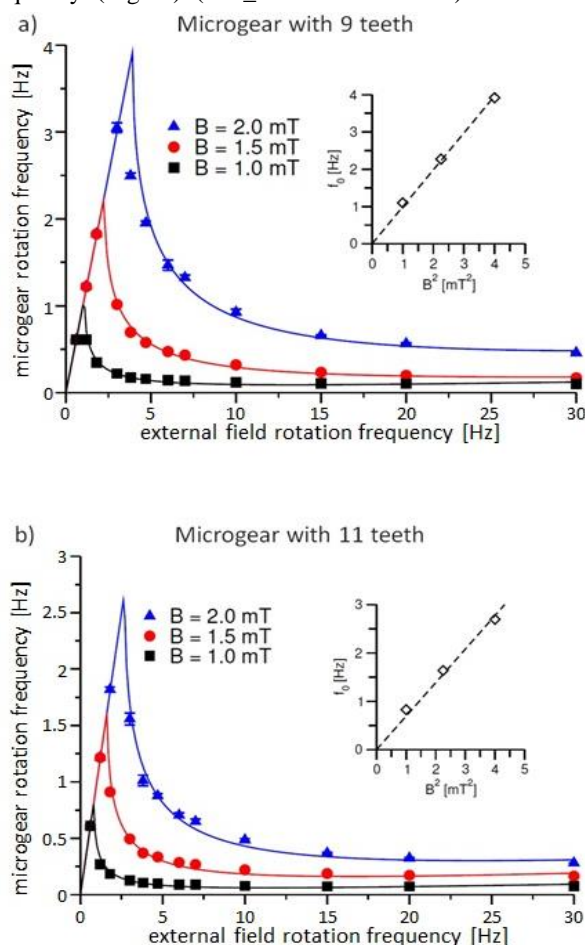


Figure 5. Rotation frequency of a single microgear with 9 teeth (a) and 11 teeth (b) as a function of the field rotation frequency for 3 different field strengths. The continuous lines show the dependence according to eq. (12), fitted to the measured data. The insets show the obtained critical frequency f_0 plotted against B^2 , confirming $f_0 \sim B^2$.

reproduced by eq. (12) and show that the microgear rotation frequency and the field frequency have the same value up to a critical frequency, after which the microgear rotation frequency decreases with increasing field frequency. The fitted critical frequencies f_0 depend quadratically on the strength of the magnetic field $f_0 \sim B^2$ as expected if the torque is caused by anisotropy and relaxation, Eq. (7).

For the same field strength the critical frequency of the larger microgear is lower than the smaller one. This can be understood as follows. The rotational drag coefficient due to a thin viscous layer between a rotating disc and a surface scales with the fourth power of the radius, $\gamma \sim r^4$. With the volume of a microgear $V \sim r^2$ and the assumption that the numerical anisotropy ε is independent of r , Eq. (7) predicts $\omega_0 \sim r^{-2}$. This would mean that the critical frequencies of the 9- and 11-tooth microgear should differ by a factor of 1.39, which is in good agreement with the measured ratio (Fig. 5) of 1.43.

D Meshed magnetic and non-magnetic microgear

By combining magnetic and non-magnetic microgears more complex configurations can be realized. In the simplest case of two microgears the magneto-responsive gear acted as power-unit for the non-magnetic gear. Fig. 6a shows the rotation

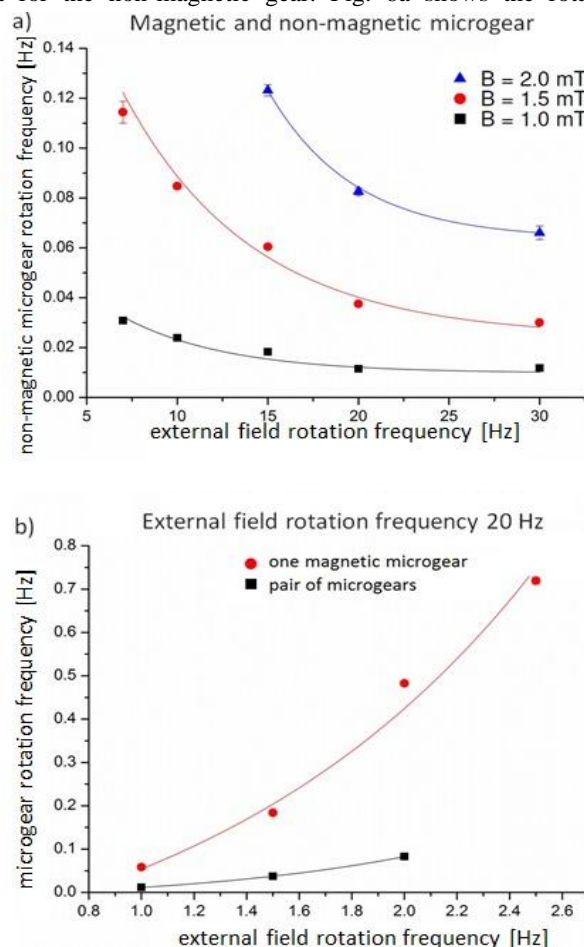


Figure 6. a) Rotation frequency of a pair of microgears (one magnetic and one non-magnetic) with 9 teeth as a function of the field rotation frequency for different field strengths. b) comparison of the microgear (circles: one magnetic; squares: pair of microgears) rotation frequency as a function of the field strength for a field rotation frequency 20 Hz.

frequency of a pair of meshed microgears (9 teeth) for various field strengths (1, 1.5 and 2 mT), as a function of the applied field frequency.

Fig. 6b shows the microgear rotation frequency (circles - one magnetic microgear and squares - pair of microgears) as a function of the magnetic field strength for the field rotation frequency 20 Hz. The rotation frequency for a pair of microgears is lower than for a single microgear (ESI_5: movie5, movie6). According to Eq. (7) both R and ω_o (and f_o) are inversely proportional to the drag coefficient γ . One can expect the drag coefficient of two coupled gears to be at least 2γ , which would lead to parameters $R/2$ and $f_o/2$. Eq. (12) would then predict that the frequency of two gears should be $1/2$ that of a single gear at high frequencies and $1/4$ at intermediate. In reality the frequency reduction in the presence of a second gear is somewhat higher (Fig. 6b), indicating that the meshed gears have a higher friction coefficient, or possibly an additional elastic interaction which is not included in the model. More complex configurations could be realized by adding further microgears (ESI_5: movie7).

IV. Conclusions

We have shown that the fabrication of highly magneto-responsive nonspherical microparticles using photo- and soft lithography has the prospect for a number of new materials-based applications. We demonstrated a potential microfluidic application of such microparticles by producing magneto-responsive microgears. These microgears can be driven with a rotating magnetic field. The gear rotation frequency shows a non-monotonous dependence on the field frequency. At low frequencies the gear is phase locked to the field. Above a critical frequency phase slippage occurs and the rotation frequency decreases with increasing field frequency. A simple model reproduces both dynamical regimes. We also demonstrated that magnetic microgears together with non-magnetic ones can be assembled into microtransmissions.

Acknowledgements

The authors acknowledge funding by the European Union Seventh Framework Program (FP7) ITN Marie Curie and the Slovenian Research Agency, grant J1-5437. The authors also thank the company Nanos Scientifacae d.o.o. (Nanos Sci.; www.nanos-sci.com) for kindly provided magnetic PDMS (sSPIONs™|PDMS) and superparamagnetic nanoclusters (iNANOvative™|silica), Dr Petar Panjan from Department of Thin Films and Surfaces (IJS) who prepared the nickel coated substrates, as well as Uroš Jorgačevski who manufactured the aluminium frames.

Notes and references

^a Faculty of Mathematics and Physics, University of Ljubljana, Jadranska 19, 1000 Ljubljana, Slovenia; E-mail: ivnakavre@gmail; dusan.babic@fnf.uni-lj.si

^b Nanos Scientifacae d.o.o. (Nanos Sci), Teslova 30, 1000 Ljubljana, Slovenia; E-mail: slavko.kralj@ijs.si

^c Department of Material Synthesis, Jožef Stefan Institute, Jamova 39, 1000 Ljubljana, Slovenia; E-mail: slavko.kralj@ijs.si

^d Department of Condensed Matter Physics, Jožef Stefan Institute, Jamova 39, 1000 Ljubljana, Slovenia; E-mail: andrej.vilfan@ijs.si

† Electronic Supplementary Information available: experimental details and movies. See DOI: 10.1039/b000000x/

- 1 A. K. Gupta, M. Gupta, *Biomaterials*, 2005, **26**, 3995
- 2 Q. A. Pankhurst, J. Connolly, S. K. Jones, J. Dobson, *J. Phys. D: Appl. Phys.*, 2003, **36** R167
- 3 P. A. Voltiras, D. I. Fotiadis, L. K. Michalis, *J. Biomech.*, 2002, **35**, 813
- 4 L. Mair, K. Ford, M. R. Alam, R. Kole, M. Fisher, R. Superfine, *J. Biomed. Nanotechnol.*, 2009, **5**, 182
- 5 L. He, M. Wang, J. Ge, Y. Yin, *Acc. Chem. Res.*, 2012, **45**, 1431
- 6 Y. Lu, Y. Yin, Y. Xia, *Adv. Mater.*, 2001, **13**, 415
- 7 J. H. Lee, J. W. Jun, S. I. Yeon, J. S. Shin, J. Cheon, *Angew. Chem.*, 2006, **118**, 8340; *Angew. Chem. Int. Ed.*, 2006, **45**, 8160
- 8 Y. Hu, L. He, Y. Yin, *Small*, 2012, **8**, 3795
- 9 B. Kavcic, D. Babic, N. Osterman, B. Podobnik, I. Poberaj, *Appl. Phys. Lett.*, 2009, **95**, 023504
- 10 J. M. Ng, I. Gitlin, A.D. Stroock, G. M. Whitesides, *Electrophoresis*, 2002, **23**, 3461
- 11 P. Tierno, R. Golestanian, I. Pagonabarraga, F. Sagues, *Phys. Rev. Lett.*, 2008, **101**, 218304
- 12 A. Ghosh, P. Fischer, *Nano Lett.*, 2009, **9**, 2243
- 13 M. Wang, L. He, Y. Yin, *Mater. Today*, 2013, **16**, 110
- 14 M. Vilfan, A. Potočnik, B. Kavčič, N. Osterman, I. Poberaj, A. Vilfan, D. Babič, *Proc. Natl. Acad. Sci. U.S.A.*, 2010, **107**, 1844
- 15 D. Babič, C. Schmitt, C. Bechinger, *Chaos* 2005, **15**, 026114
- 16 J. M. Brader, R. Evans, M. Schmidt, *Mol. Physics*, 2003, **101**, 3349
- 17 T. Sawetzki, S. Rahmouni, C. Bechinger, D. W. M. Marr, *Proc. Natl. Acad. Sci. U.S.A.*, 2008, **105**, 20141
- 18 G. Kokot, M. Vilfan, N. Osterman, A. Vilfan, B. Kavčič, I. Poberaj, D. Babič, *Biomeicrofluidics*, 2011, **5**, 034103
- 19 C. F. Brooks, G. G. Fuller, C. W. Frank, C. R. Robertson, *Langmuir*, 1999, **15**, 2450
- 20 M. Adams, Z. Dogic, S. L. Keller, S. Fraden, *Nature*, 1998, **393**, 349
- 21 A. Donev, F. H. Stillinger, P. M. Chaikin, S. Torquato, *Phys. Rev. Lett.*, 2004, **92**, 255506
- 22 B. Mihiretie, J. C. Loudet, B. Pouligny, *Europhys. Lett.*, 2012, **100**, 48005
- 23 J. Zhu, R. C. Hayward, *J. Am. Chem. Soc.*, 2008, **130**, 7496
- 24 J. H. Park, G. von Maltzahn, L. Zhang, M. P. Schwartz, E. Ruoslahti, S. N. Bhatia, M. J. Sailor, *Adv. Mater.*, 2008, **20**, 1630
- 25 S. Q. Choi, S. G. Jang, A. J. Pascall, M. D. Dimitriou, T. Kang, C. J. Hawker, T. M. Squires, *Adv. Mater.*, 2011, **23**, 2348
- 26 B. Wang, H.C. Shum, D.A. Weitz, *Chem. Phys. Chem.*, 2009, **10**, 641
- 27 D. K. Hwang, D. Dendukuri, P. S. Doyle, *Lab Chip*, 2008, **8**, 1640
- 28 J. Nunes, K. P. Herlihy, L. Mair, R. Superfine, J. M. DeSimone, *Nano Lett.*, 2010, **10**, 1113
- 29 S. Y. Lee, S. Yang, *Angew. Chem.*, 2013, **31**, 8318; *Angew. Chem. Int. Ed.*, 2013, **52**, 8160
- 30 J.W. Tavacoli, P. Bauër, M. Fermigier, D. Bartolo, J. Heuvingh, O. du Roure, *Soft Matter*, 2013, **9**, 9103
- 31 R. Menon, A. Patel, D. Gil, H. I. Smith, *Mater. Today*, 2005, **8**, 26
- 32 B. Kavcic, D. Babic, N. Osterman, B. Podobnik, I. Poberaj, *Microsyst. Technol.*, 2012, **18**, 191
- 33 Y. Xia, G. M. Whitesides, *Annu. Rev. Mater. Sci.*, 1998, **28**, 153
- 34 B. D. Gates, Q. Xu, M. Stevart, D. Ryan, C. G. Willson, G. M. Whitesides, *Chem. Rev.*, 2005, **105**, 1171
- 35 Y. Xia, J. Tien, D. Qin, G. M. Whitesides, *Langmuir*, 1996, **12**, 4033
- 36 I. Wong, C.-M. Ho, *Microfluid Nanofluidics*, 2009, **7**, 291
- 37 B. Navinšen, J. Fine, *Vacuum*, 1986, **36**, 711
- 38 G. Helgesen, P. Pieranski, A.T. Skjeltrop, *Phys. Rev. Lett.*, 1990, **64**, 1425
- 39 P. Tierno, J. Claret, F. Sagues, and A. Cēbers, *Phys. Rev. E*, 2009, **79**, 021501
- 40 X. J. A. Janssen, A. J. Schellekens, K. van Ommering, L. J. van IJzendoorn, M. W. J. Prins, *Biosens. Bioelectron.*, 2009, **24**, 1937
- 41 J. Happel, H. Brenner; *Low Reynolds number hydrodynamics: With special applications to particulate media*, Springer, 1983
- 42 K. I. Morozov, A. Leshansky, *Nanoscale*, (2014), DOI: 10.1039/C4NR02953D Accepted Manuscript